

# Modeling Complexes of the Uranyl Ion $\text{UO}_2\text{L}_2^{n+}$ : Binding Energies, Geometries, and Bonding Analysis

Carine Clavaguéra-Sarrio, Sophie Hoyau, Nina Ismail, and Colin J. Marsden\*

Laboratoire de Physique Quantique, IRSAMC, Université Paul Sabatier, 118 route de Narbonne, 31 062 Toulouse Cedex 4, France

Received: October 18, 2002; In Final Form: February 17, 2003

A systematic study has been carried out with density functional theory of  $\text{UO}_2\text{L}_2^{n+}$  ( $n = 0$  or  $2$ ) complexes. Thirty three ligands have been considered, enabling a large database of binding energies and geometries to be established that can improve our knowledge and understanding of the bonding between the uranyl ion  $\text{UO}_2^{2+}$  and potential ligands or solvent. A statistical study has been performed using the database with the twin aims of predicting the coordination energies of new complexes and revealing the dominant bonding parameters. We have shown that it is possible to predict the coordination energy satisfactorily just from the properties of the isolated ligand. However, the statistical analysis is shown to be physically unsound. To develop our understanding of the nature of the uranyl–ligand bond, the coordination energy has been decomposed into several contributions: electrostatic, repulsion, ligand polarization, uranyl polarization, charge transfer from the ligand to the uranyl ion, and inverse charge transfer. It is clear that the electrostatic term cannot be modeled just by the ligand's dipole moment; a multipole development extending at least to the quadrupole moment is necessary. Our quantitative analysis also shows that the polarization and charge-transfer terms are important and must be included in any force field if numerically and physically reliable results are sought.

## (I) Introduction

Actinide chemistry is an active field of research at present, for both fundamental and applied reasons. The coordination chemistry of the actinides is fascinating, rich, and quite different from that of the transition metals. Given the increasing quantities of nuclear waste that must be treated, an improved knowledge of the coordination of the actinides becomes increasingly urgent. In view of the problems posed by radioactivity, systematic experimental studies of the actinides are not easy. Until recently, there have been very few theoretical studies of actinide chemistry, since the large number of electrons to be treated and the critical influence of relativistic effects posed very severe technical problems. However, the dramatic recent advances in both computing technology and methodology mean that it is now possible to undertake reliable theoretical studies of molecular systems containing an actinide and a limited number of other atoms, with the aim of both supplying selected data that are not presently available from experiments and developing our understanding of the nature of the fundamental aspects of actinide coordination chemistry. The dominant form of uranium in nuclear waste is the uranyl ion  $\text{UO}_2^{2+}$ . The waste is treated in the aqueous phase, and uranium is typically surrounded by five ligand atoms in the “equatorial” plane that is perpendicular to the  $\text{O}=\text{U}=\text{O}$  axis. Interactions between a water molecule and a  $2+$  cation are both strong and of a long range. A realistic theoretical treatment of these systems will therefore necessitate a satisfactory account of these interactions beyond the first coordination sphere of the uranium atom. These considerations show that it is not feasible at present to undertake detailed quantum calculations on a complete experimental system, so as to be able to compare directly with experiments undertaken

in aqueous solution.<sup>1</sup> It is therefore necessary to study model systems in order to understand the chemistry of uranium in more detail.

In previous calculations,<sup>2</sup> some systematic studies were carried out of the uranyl ion surrounded by halide anions, water, or  $\text{H}_2\text{S}$  molecules; systems containing one to five ligands were treated. We report here a study of  $\text{UO}_2\text{L}_2^{n+}$  systems. We have considered 33 different ligands, mostly neutral molecules but some anionic. The donor atom is one of N, O, F, P, S, Cl, Br, and I. The choice of  $\text{UO}_2\text{L}_2^{n+}$  systems was influenced by two factors. First, it is clearly simpler to study a small system than a large one, and systems of the type  $\text{UO}_2\text{L}_5$  would have required a much greater investment in computing resources. But second, the even simpler choice of  $\text{UO}_2\text{L}$  systems would preclude any analysis of “three-body” effects (where we consider the uranyl ion and the ligand as single entities).  $\text{UO}_2\text{L}_2^{n+}$  species are, therefore, the simplest that enable us to extract the information that we require. Even though they are model systems, they will allow us to analyze correctly the differences in bonding between different ligands and to show the importance, both relative and absolute, of the different effects that we wish to quantify.

The first question we considered was the variation of the binding energy with the nature of the ligand. What are the factors that lead to particularly stable complexes? An answer to this question should be useful in planning improvements to treatment of nuclear waste. A second question follows from the first: can we predict the binding energy of a ligand to the uranyl ion just from the properties of the isolated ligand? If so, which properties of the ligand are most influential? To provide answers to these questions, we have undertaken statistical fits by least squares. The third area of this work involves a detailed study of the nature of the uranyl–ligand bond. We have considered partitioning the coordination energy into its main components: the electro-

\* Corresponding author. E-mail: colin.marsden@irsamc.ups-tlse.fr. Fax: (+33) 5 61 55 60 65.

static and repulsion terms that appear in classical force fields, and also the polarization and charge-transfer terms that are more difficult to model but which we suspect to be important. Indeed, Hemmingsen and co-workers<sup>3</sup> have recently emphasized the inadequacy of standard force fields and the need to include both polarization and charge-transfer effects in a realistic model potential.

Guilbaud et al.<sup>4</sup> have presented molecular dynamics (MD) calculations for the uranyl ion and its environment. They used the Amber 4.0 force field<sup>5</sup> and a simple 1–6–12 potential without polarization and charge transfer terms. To our knowledge this is the only MD test for these systems. As mentioned by Hemmingsen et al.,<sup>3</sup> a more sophisticated potential is essential to describe more completely the bonding in uranyl complexes. Our goal is to establish simple yet reliable relationships to model both polarization and charge transfer in uranyl complexes. A correct analysis of the nature of ligand–uranyl interactions in small complexes will allow the dominant terms to be identified and modeled analytically. While this analysis is performed for gas-phase systems, for reasons of simplicity, its conclusion, if correct, will allow us in subsequent work to develop a model potential that will be appropriate for the uranyl ion in aqueous solution; the long-range effects due to water molecules in the second and subsequent hydration shells will be included explicitly.

The structure of this paper is as follows. In section II, we summarize the computational methods and basis sets that we have used. We also present the method developed for analyzing ligand binding energies. The section III (Results and Discussion) begins with a presentation of the database we have developed for the uranyl complexes: geometries, vibrational frequencies, binding energies, and charge transfer are reported and analyzed. A statistical study of the QSAR type is then presented. We conclude with a detailed analysis of the various components of the binding energies, expressed as physically meaningful quantities. Analytical expressions for these components are developed and successfully tested.

## (II) Computational Methods

For all the uranyl complexes, full geometry optimizations and natural bond orbital (NBO) population analyses<sup>6</sup> have been performed at both Hartree–Fock and density functional theory (DFT) levels, using the B3LYP<sup>7</sup> hybrid functional. Analytical vibrational frequency computations have been carried out to confirm that the structures obtained are minima on the potential energy surface. The basis set superposition error (BSSE) has been evaluated in selected cases by the counterpoise method.<sup>8</sup> The magnitude of this error is typically 5 kJ/mol, that is, of the order of only 1% of the interaction energy, and we, therefore, judged these errors to be negligible. These calculations have been carried out using the Gaussian 98 code.<sup>9</sup>

To determine the various contributions to the interaction energy, the Molcas 5.0 package<sup>10</sup> has been used to perform a coordination energy partitioning (CEP) at the Hartree–Fock level (see Section II.2).

For the sake of consistency, effective core potentials (ECPs) and associated basis sets of similar quality have been used for all atoms of the ligands in both Gaussian and Molcas packages.

**(1) Basis Sets and ECPs.** In a previous calibration study,<sup>11</sup> Ismail et al. have shown that the use of a “Stuttgart” relativistic effective core potential (RECP)<sup>12</sup> for the uranium atom, together with a slightly modified basis set, leads to a description of the uranyl ion which is very similar to that obtained in four-component calculations at several levels of theory.<sup>13</sup> This is a

“very small core” RECP where 32 electrons are treated explicitly [5s<sup>2</sup>5p<sup>6</sup>5d<sup>10</sup>5f<sup>5</sup>6s<sup>2</sup>6p<sup>6</sup>6d<sup>1</sup>7s<sup>2</sup>].

For atoms such as C, N, O, S, P, F, Cl, and Br, the ECPs developed in ref 14 have been used. The associated basis sets are of at least “double  $\zeta$ ” quality<sup>2b,c</sup> (see below). For I, relativistic effects have to be taken into account, and a Stuttgart RECP associated with a “double  $\zeta$  plus polarization plus diffuse” basis set has been chosen. For the hydrogen atom, a basis set of “double  $\zeta$ ” quality has been used. In all cases, polarization and diffuse functions have been added to the coordination center basis set to improve the description of the interaction with the uranyl ion. The number and size of molecular systems studied in this work limit severely the theoretical methods that could be used. From extensive tests on the [UO<sub>2</sub>(H<sub>2</sub>O)]<sup>2+</sup> complex, we were able to show, first, that the ligand binding energy predicted by the B3LYP method is close to that obtained with more rigorous but much more expensive methods such as CCSD and, second, that the B3LYP binding energy varies only slightly if larger bases than those detailed above are employed.

In CEP calculations, Stuttgart RECPs<sup>15</sup> have been used for all atoms, as the Toulouse ECPs are not implemented in Molcas. In each case, the associated basis set has been augmented with a diffuse function, so that it was comparable to the Toulouse basis set. The use of these two different RECPs and associated basis sets has been shown to lead to negligible differences in selected cases in both binding energies and geometries.

**(2) Coordination Energy Partitioning.** The “reduced variational space” self-consistent field (RVS SCF) method was first proposed by Fink<sup>16</sup> to evaluate the various contributions to the interaction energy in any system composed of two entities. It relies on the use of SCF-optimized monomer molecular orbitals (MOs) in dimer calculations. The function space is divided so that the MOs of one fragment may be optimized in the field of the frozen MOs of the other. In addition, the variational space may be truncated by removing the unoccupied orbitals of either fragment in order to isolate polarization, charge transfer, and basis set superposition effects of each entity. This method is similar to Morokuma’s,<sup>17</sup> but it can in principle be used at both HF and DFT levels. For the moment, only the Hartree–Fock decomposition can be performed. However, as discussed in more detail in section III.2, interaction energies of the uranyl complexes are rather similar at the HF and B3LYP levels.

In our case, the RVS decomposition allows us to determine the sum of the electrostatic and repulsion contributions (ELEC + REP), the polarization of the ligand by the uranyl ion (POL<sub>L</sub>), the polarization of the uranyl ion by the ligand (POL<sub>C</sub>), the charge transfer from the ligand to the uranyl ion (CT<sub>L→C</sub>), and the charge transfer from the uranyl ion to the ligand or inverse charge transfer (CT<sub>C→L</sub>). Details on the computation of each term are presented in Scheme 1. ELEC (and hence REP) can be determined by replacing the cation with a point charge.<sup>18</sup> The ligand polarization can also be estimated using this simple “point charge” method; however, the POL<sub>L</sub> contribution determined in this way is severely exaggerated at short distances, as the screening effects due to the electronic cloud of the cation are not taken into account.

In all of these computations the ligand and the uranyl ion have been considered in the geometry of the complex. Since the deformation energy of the fragments in the complex corresponds to less than 1% of the interaction energy, similar results would be obtained using optimized monomer geometries.

## (III) Results and Discussion

**(1) Database: Geometries, Frequencies, Binding Energies, and Charge Transfer.** The database for the UO<sub>2</sub>L<sub>2</sub><sup>n+</sup> complexes

**SCHEME 1. Coordination Energy Partitioning: RVS (Reduced Variational Space) Method**

MO basis set	Contribution
$C_{\text{occ}} + L_{\text{occ}}$	$E_L + E_C + \text{REP} + \text{ELEC} \rightarrow$ <b>point charge model</b> (1 <sup>st</sup> iteration)
<b>Ligand (L)</b>	
$[C_{\text{occ}}] + L_{\text{occ}} + L_{\text{vac}}$	$E_L + E_C + \text{REP} + \text{ELEC} + \text{POL}_L$ $\Rightarrow$ <b>POL<sub>L</sub></b>
$[C_{\text{occ}}] + L_{\text{occ}} + C_{\text{vac}} + L_{\text{vac}}$	$E_L + E_C + \text{REP} + \text{ELEC} + \text{POL}_L + \text{CT}_{L \rightarrow C} + \text{BSSE}_L$ $\Rightarrow$ <b>CT<sub>L→C</sub> + BSSE<sub>L</sub></b>
<b>Uranyl Cation (C)</b>	
$[L_{\text{occ}}] + C_{\text{occ}} + C_{\text{vac}}$	$E_L + E_C + \text{REP} + \text{ELEC} + \text{POL}_C$ $\Rightarrow$ <b>POL<sub>C</sub></b>
$[L_{\text{occ}}] + C_{\text{occ}} + L_{\text{vac}} + C_{\text{vac}}$	$E_L + E_C + \text{REP} + \text{ELEC} + \text{POL}_C + \text{CT}_{C \rightarrow L} + \text{BSSE}_C$ $\Rightarrow$ <b>CT<sub>C→L</sub> + BSSE<sub>C</sub></b>
[ ] are frozen orbitals	

is given in Table 1. L can be an anionic or a neutral ligand, so  $n$  equals 0 or 2. We report coordination energies, geometric parameters related to the complexation,  $\Delta\nu$  symmetric and antisymmetric (the difference between the free and complexed uranyl ion vibrational frequencies), and NBO charge transfers. The coordination energies and NBO charge transfers have been computed as follows:

$$E_{\text{coord}} = E_{\text{comp}} - 2^*E_L - E_{\text{uranyl}}$$

$$\text{CT (NBO)} = 2 - q_{\text{NBO}}(\text{U}) - 2^*q_{\text{NBO}}(\text{O})$$

We now supply a few details concerning the geometries of the  $\text{UO}_2\text{L}_2^{n+}$  complexes, as the data in Table 1 are not always

sufficient to define the structures completely. Note that three of the complexes are represented in Figure 1. The U–L distance given in Table 1 for  $[\text{UO}_2(\text{H}_2)_2]^{2+}$  refers to the center of mass of the  $\text{H}_2$  molecules, which are oriented perpendicular to the equatorial plane of the uranyl ion. The H–H distance in the complex is increased by 0.026 Å compared to that in free  $\text{H}_2$ . CO binds to  $\text{UO}_2^{2+}$  through C, with the two CO groups lying in the equatorial plane. The U–C–O angle is essentially 180°. No minimum could be found with CO bound through O. An analogous structure is found for the NO complex, which is a triplet.

The HCl groups in  $\text{UO}_2(\text{HCl})_2$  are essentially antiparallel, that is, with O–U–Cl–H dihedral angles of almost zero. The U–Cl–H angle is 106.5°. However, in the HF species the U–F–H units are almost linear. These two structures are discussed further in section III.3.  $\text{CO}_2$  binds to the uranyl ion through an oxygen atom. The U–O–C angle is essentially 180°. The C=O group bonded to U is lengthened by 0.035 Å compared to the case of free  $\text{CO}_2$ . The  $[\text{UO}_2(\text{H}_2\text{S})_2]^{2+}$  complex has an intriguing structure with only  $C_s$  symmetry. The  $\text{H}_2\text{S}$  units make an angle of 70° with the  $\text{UO}_2$  plane; although the two  $\text{H}_2\text{S}$  groups are not equivalent, the structural differences between them are very minor.

For each  $\text{H}_2\text{S}$  molecule, one localized lone pair points toward the U atom; the other is roughly parallel to the S–U–S bisector in one case but parallel to the other U–S bond for the second. This structure is discussed in detail in section III.3. A second structure for  $[\text{UO}_2(\text{H}_2\text{S})_2]^{2+}$  was located which is also a minimum. It has  $C_{2v}$  symmetry and is only 2 kJ/mol less stable than the first. The MeCl and MeF complexes adopt conforma-

**TABLE 1: Database for  $\text{UO}_2\text{L}_2^{n+}$  Complexes: Symmetry Point Group of the Complex, Coordination Energy, Uranium–Ligand Distance, Ligand–Uranium–Ligand Angle, Deviation from the Uranyl Distance, Deviation from the Uranyl Frequencies (Symmetric and Antisymmetric), and NBO Charge Transfer from the Ligand to the Uranyl Ion (Electrons)**

ligand <sup>a</sup>	symm point group	$E_{\text{coord}}$ (kJ/mol)	$r(\text{U–L})$ (Å)	ang(L–U–L) (deg)	$\Delta r(\text{U=O})$ (Å)	$\Delta\nu(\text{U=O})_{\text{antisym}}$ ( $\text{cm}^{-1}$ )	$\Delta\nu(\text{U=O})_{\text{sym}}$ ( $\text{cm}^{-1}$ )	CT (NBO)
$\text{H}_2$	$C_{2v}$	131	2.49	108.5	0.009	21	13	0.14
CO	$C_{2v}$	268	2.71	109.0	0.015	35	26	0.25
NO	$C_{2v}$	305	2.64	120.4	0.031	67	79	0.20
HCl	$C_2$	335	2.81	104.1	0.020	46	37	0.41
HF	$C_2$	338	2.40	122.3	0.013	30	25	0.13
$\text{CO}_2$	$C_{2v}$	349	2.39	119.0	0.019	44	39	0.19
$\text{H}_2\text{S}$	$C_s$	461	2.88	104.5	0.027	18	29	0.53
MeCl	$C_2$	486	2.72	103.8	0.028	64	54	0.50
$\text{PH}_3$	$C_{2v}$	502	2.99	108.6	0.027	66	38	0.56
MeF	$C_2$	524	2.27	118.9	0.025	57	48	0.25
$\text{H}_2\text{O}$	$C_{2v}$	551	2.36	110.7	0.025	51	44	0.25
HCN	$C_{2v}$	563	2.44	108.5	0.023	53	43	0.21
$\text{OC}_4\text{H}_4$	$C_{2v}$	589	2.33	113.2	0.037	82	76	0.42
$\text{OCH}_2$	$C_{2v}$	608	2.31	121.0	0.029	63	56	0.30
$\text{NH}_3$	$C_2$	627	2.50	106.9	0.028	58	49	0.30
$\text{Me}_2\text{S}$	$C_{2v}$	677	2.70	114.4	0.042	94	87	0.76
MeCN	$C_2$	697	2.39	109.4	0.029	66	54	0.26
pyrazine	$C_{2v}$	697	2.42	105.9	0.040	90	83	0.41
OMe <sub>2</sub>	$C_{2v}$	718	2.29	116.3	0.039	85	73	0.40
SPH <sub>3</sub>	$C_2$	755	2.70	103.5	0.046	116	101	0.81
PMe <sub>3</sub>	$C_{2v}$	760	2.92	113.0	0.041	95	87	0.81
NMe <sub>3</sub>	$C_{2v}$	772	2.46	174.0	0.047	105	99	0.60
$\text{O}(\text{CH}_3)_2$	$C_2$	792	2.25	122.0	0.038	85	76	0.39
pyridine	$C_{2v}$	824	2.39	107.6	0.043	97	79	0.43
OPH <sub>3</sub>	$C_{2v}$	857	2.24	116.2	0.040	91	90	0.36
OPMe <sub>3</sub>	$C_{2v}$	1047	2.20	119.2	0.051	115	123	0.46
$\text{I}^-$	$C_{2v}$	1939	2.92	105.1	0.061	135	122	1.12
$\text{CN}^-$	$C_{2v}$	2023	2.38	107.0	0.053	119	103	0.63
$\text{Br}^-$	$C_{2v}$	2042	2.68	115.8	0.049	112	98	0.81
$\text{NC}^-$	$C_{2v}$	2064	2.25	108.5	0.059	132	115	0.53
$\text{Cl}^-$	$C_{2v}$	2089	2.54	107.9	0.062	139	120	0.82
$\text{F}^-$	$C_{2v}$	2417	2.08	114.0	0.071	159	131	0.64
$\text{OH}^-$	$C_2$	2528	2.12	111.1	0.084	183	155	0.75

<sup>a</sup> The interaction center is in italic type if the ligand has several potential binding sites.

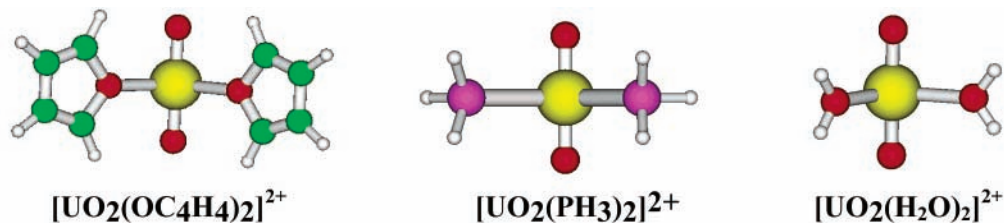


**Figure 1.** B3LYP geometries of three complexes:  $[\text{UO}_2(\text{OC}_4\text{H}_4)_2]^{2+}$ ,  $[\text{UO}_2(\text{PH}_3)_2]^{2+}$ , and  $[\text{UO}_2(\text{H}_2\text{O})_2]^{2+}$ .

tions that are very similar to those of their HX parents, though the U–Cl distance is almost 0.1 Å shorter in the methyl complex than that for  $[\text{UO}_2(\text{HCl})_2]^{2+}$ . HCN binds to uranyl through N, with effectively linear U–N–C and N–C–H units. In the formaldehyde complex all the ligand atoms lie in the equatorial plane, and the local  $C_2$  ligand axes point essentially straight at the U atom. However, the furan, pyrazine, and pyridine rings all prefer to be perpendicular to the equatorial plane.

The  $\text{H}_2\text{O}$  ligand also adopts a perpendicular orientation with respect to the equatorial plane, as does dimethyl ether. This structural preference is discussed in detail elsewhere.<sup>2c</sup> Ammonia could give a complex with  $C_{2v}$  symmetry, if one N–H bond for each  $\text{NH}_3$  lay in the equatorial plane. In fact, there is a very minor rotation (just  $7^\circ$ ) about the N–U directions of the two  $\text{NH}_3$  groups to give only  $C_2$  symmetry, though the related  $\text{PH}_3$ ,  $\text{NMe}_3$ , and  $\text{PMe}_3$  ligands all give complexes with  $C_{2v}$  symmetry. The lowest vibrational frequencies of these complexes, which correspond to torsional motion of the  $\text{ER}_3$  groups (E = N or P; R = H or  $\text{CH}_3$ ) about the U–E axes are all very low, of the order of 10–30  $\text{cm}^{-1}$ .

In the phosphine oxide complexes  $[\text{UO}_2(\text{OPH}_3)_2]^{2+}$  and  $[\text{UO}_2(\text{OPMe}_3)_2]^{2+}$ , the O and P atoms both lie in the equatorial plane and the U–O–P angles are essentially  $180^\circ$ . But in the analogous phosphine sulfide, the symmetry is reduced to  $C_2$ ; the P=S bonds are essentially parallel to the uranyl bonds, and the U–S–P angle is close to  $110^\circ$ , giving a structure rather similar to that of the HCl complexes. The cyanide ion can coordinate to uranyl either through N or through C. Both possibilities give rise to true minima, with the isocyanide being some 40 kJ/mol more stable. In both cases the C and N atoms both lie in the equatorial plane, and the U–N–C and U–C–N angles are essentially  $180^\circ$ .

In Table 2, we present computed values of several ligand properties: the dipole moment, the polarizability, the HOMO and LUMO energies, and the proton affinity (without thermodynamic corrections). Even though reliable experimental values are available for many of these quantities, the aim of our study was to investigate whether purely theoretical methods can be used to provide quantitatively useful data. Since no experimental values are available for ligand binding energies, for the sake of consistency, we wish to use theoretical values throughout. The geometry of  $[\text{UO}_2\text{L}_2]^{n+}$  is nearly always similar with an angle LUL of about  $110$ – $120^\circ$ . This observation reminds us of similar geometries already reported for complexes of  $\text{Ba}^{2+}$  or  $\text{Ca}^{2+}$  with two water molecules.<sup>19</sup> It might be thought that two ligands located in the equatorial plane of the uranyl ion would prefer to bind in a linear form, to minimize steric effects. The preferred bent geometry is attributed to core polarization of the central cation<sup>19</sup> and a competition between the dipole moment role of the ligands and the polarization energy of the uranyl ion.<sup>20</sup> We observe that the energy depends only weakly on the LUL angle; for example, in  $[\text{UO}_2(\text{H}_2\text{O})_2]^{2+}$ , the linear geometry is only 7 kJ/mol higher than the minimum, where the angle is  $111^\circ$ .  $[\text{UO}_2(\text{NMe}_3)_2]^{2+}$  is the only complex whose geometry does not obey the trend above. The N–U–N angle is  $174^\circ$  at the B3LYP level,

**TABLE 2: Database for  $\text{UO}_2\text{L}_2^{n+}$  Complexes: HOMO Energy, LUMO Energy, Proton Affinity, Dipole Moment, and Polarizability of the Ligand<sup>a</sup>**

ligand	$E_{\text{HOMO(L)}}$ (eV)	$E_{\text{LUMO(L)}}$ (eV)	PA (kJ/mol)	dipole moment (D)	polarizability ( $\text{au}^3$ )
$\text{H}_2$	–11.60	0.12	440	0	0.8
CO	–10.57	–0.04	595	0.00	15.7
NO	–6.47	–0.12	528	0.02	14.8
HCl	–9.22	0.00	557	1.48	13.4
HF	–11.49	0.00	483	2.08	5.0
$\text{CO}_2$	–10.40	0.01	541	0	26.5
$\text{H}_2\text{S}$	–7.23	0.01	728	1.36	17.1
MeCl	–8.20	0.00	650	2.29	30.1
$\text{PH}_3$	–7.66	–0.01	794	1.00	22.3
MeF	–9.60	0.05	623	2.42	14.5
$\text{H}_2\text{O}$	–8.69	0.04	709	2.24	6.5
HCN	–10.05	0.01	715	3.06	22.1
$\text{OC}_4\text{H}_4$	–8.83	0.01	728	0.94	48.4
OCH <sub>2</sub>	–7.63	–0.06	732	2.58	21.1
$\text{NH}_3$	–7.28	0.01	886	1.83	12.0
Me <sub>3</sub> S	–5.94	0.01	850	1.81	40.5
MeCN	–9.15	0.03	788	4.08	37.1
pyrazine	–7.16	–0.06	904	0	62.6
OMe <sub>2</sub>	–6.95	0.08	834	1.75	26.3
SPH <sub>3</sub>	–6.65	–0.04	834	4.18	58.8
PMe <sub>3</sub>	–6.07	0.01	976	1.48	53.1
NMe <sub>3</sub>	–5.69	0.05	998	0.92	40.2
O(CH <sub>3</sub> ) <sub>2</sub>	–6.99	–0.02	837	3.37	43.6
pyridine	–7.15	–0.03	964	2.54	67.1
OPH <sub>3</sub>	–8.06	–0.03	838	4.15	29.5
OPMe <sub>3</sub>	–7.10	–0.01	868	4.87	57.7
$\text{I}^-$	–0.89	0.19	1303	0	31.0
$\text{CN}^-$	–1.28	0.19	1477	0.69	34.5
$\text{Br}^-$	–1.97	0.21	1262	0	11.6
$\text{NC}^-$	–1.28	0.19	1420	0.69	34.5
$\text{Cl}^-$	–0.81	0.24	1370	0	14.4
$\text{F}^-$	+0.04	0.30	1560	0	7.3
$\text{OH}^-$	+1.09	0.30	1637	2.06	10.9

<sup>a</sup> The interaction center is in italic type if the ligand has several potential binding sites.

but we have not been able to find a satisfactory rationalization for this anomaly. A “typical” N–U–N angle of  $120^\circ$  would not lead to any undue steric distress between the two  $\text{NMe}_3$  ligands, and in fact the angle is  $125^\circ$  at the SCF level of theory.

The U=O distance is lengthened by coordination but only slightly. The largest change is only 0.084 Å. There is a clear tendency for the change in the uranyl bond length to increase with the binding energy of the ligand, but the correlation is certainly not perfect. As the change of the uranyl distance induced by the ligand coordination is relatively small, we may conclude that model potentials, in which frozen geometries are assumed,<sup>20</sup> can be safely used for these complexes.

On the other hand, the U=O symmetric and antisymmetric vibrational frequencies vary substantially with the nature of the ligand, and the decrease can be as much as 183  $\text{cm}^{-1}$  (16%). Since changes of this magnitude can easily be measured, it is tempting to inquire whether the change of vibrational frequencies can be used to determine the ligand coordination energy. However, inspection of Table 1 shows that while there is a

general tendency for the decrease of vibrational frequencies to increase with the coordination energy, the correlation is again far from perfect. In some cases, the uranyl vibrational modes also involve motion of the ligand atoms, and this vibrational mixing reduces the usefulness of the vibrational wavenumbers as a probe of the ligand binding.

The ligand coordination energies range from as little as 130 kJ/mol for  $\text{L} = \text{H}_2$  to more than 2500 kJ/mol for the anionic ligand  $\text{OH}^-$ . In any column of the periodic table, the most stable complexes are formed by the smallest donor; for example,  $\text{NH}_3$  binds more strongly than  $\text{PH}_3$ ,  $\text{H}_2\text{O}$  more strongly than  $\text{H}_2\text{S}$ , and  $\text{F}^-$  more strongly than  $\text{Cl}^-$ . These observations suggest that the uranyl ion should be regarded as a hard cation in the context of Pearson's HSAB theory.<sup>21</sup> On the other hand, since ammonia binds more strongly than water, and  $\text{PH}_3$  more strongly than  $\text{H}_2\text{S}$ , it appears that the uranyl ion is sometimes ambivalent. If the E–H bonds are replaced by E– $\text{CH}_3$  in any ligand L (E is the donor atom: N, O, F, ...), the binding energy to the uranyl ion systematically increases. These effects will be analyzed in more detail in future work. It is reassuring to note that the phosphine oxide  $\text{OPMe}_3$  is the ligand that gives the most stable complex  $\text{UO}_2\text{L}_2^{2+}$  and that the ligand used in the PUREX<sup>22</sup> treatment procedure is indeed an alkylated (tributyl) phosphine oxide.

NBO analysis shows that charge transfer to the uranyl ion is appreciable, ranging from 0.14 to 1.12 electrons for the  $\text{UO}_2\text{L}_2^{n+}$  systems considered here. We note that the formal oxidation state for uranium in the uranyl ion is very high (+VI) and the electron affinity of the uranyl ion is enormous, of the order of 15 eV.<sup>23</sup> Charge transfer from the ligand to the empty f orbitals is therefore obviously favored. In other words, the interaction between  $\text{UO}_2^{2+}$  and L has some covalent character and we may anticipate that the coordination energy will be influenced by the charge transfer as well as by the electrostatic and polarization terms.

The NBO method is not the only scheme available for determining the extent of charge transfer. Among the various population analyses that have been proposed, Mulliken's is probably the best known.<sup>24</sup> However, the numerical results yielded by Mulliken's method are very sensitive to the details of the basis set. For example, suppression of the diffuse functions from the oxygen basis in  $[\text{UO}_2(\text{H}_2\text{O})]^{2+}$  increases the charge transfer from 0.23 to 0.36 electron, even though the total energy and geometry change by only trivial amounts. The NBO estimates (0.14 electron) are numerically far more stable, changing in this example by less than 0.01 electron.

In assessing the reliability of our energy partitionings, it must be acknowledged that the basis sets used here are not large enough to yield highly accurate values for ligands' dipole moments and polarizabilities. In general, the dipole moments will be overestimated but the polarizabilities underestimated. However, we note that the calculated binding energies are scarcely altered if a larger basis is used. For example, the binding energy calculated for a single  $\text{H}_2\text{O}$  molecule is changed by only 3% if the polarization bases on O and H are increased to 3d and 2p, respectively; this basis yields excellent values of the electric moments for  $\text{H}_2\text{O}$ . We therefore anticipate that our conclusions concerning the binding energy components would be essentially unchanged if larger basis sets were used.

**(2) Statistical Study.** With the large database, a statistical study in the QSAR sense (quantitative structure–activity relationships) has been undertaken. Rabbe<sup>25</sup> first used similar methods to fit the parameters for a force field on the basis of semiempirical calculations for large uranyl complexes. The goal

**TABLE 3: Uranium–Ligand Distances Chosen for Each Coordination Center, Neutral or Anionic, in the Statistical Study ( $r$  in Angstroms)**

coordination center: neutral ligand		$r$	coordination center: anionic ligand		$r$
O		2.3	$\text{OH}^-$		2.1
N		2.45	$\text{NC}^-$		2.25
C		2.55	$\text{CN}^-$		2.35
S		2.75	$\text{F}^-$		2.1
P		2.9	$\text{Cl}^-$		2.55
F		2.3	$\text{Br}^-$		2.70
Cl		2.75	$\text{I}^-$		2.95

of that study was to understand more about the ligand selectivity of  $\text{UO}_2^{2+}$  in the waste environment, but the potential was so simple (it did not take into account the polarization and charge-transfer phenomena) that it did not yield accurate chemical estimates.

Our goal is to estimate the coordination energy as a sum of contributions, each linked to a single parameter whose physical meaning is clear. As we want to estimate the coordination energy of a new complex without undertaking lengthy calculations, we use only ligand-related parameters determined from B3LYP calculations, with the same basis as that used to establish the database.

Chemical intuition suggested the following parameters and their variations with the distance  $r$  between the uranium atom and the coordination center of the ligand:

- (i) an electrostatic term related to the charge  $q/r$  and/or to the dipole moment  $\text{DM}/r^2$
- (ii) a polarization term related to the polarizability  $\text{POL}/r^4$
- (iii) a repulsion term  $\exp(-r)$  (denoted REP)
- (iv) the proton affinity PA; this parameter was suggested by possibly naïve analogies considering the Lewis and Bronsted acidities of the ligand to be comparable
- (v) a parameter to represent the charge transfer is needed: as no expression has become well established, we decide to take the NBO charge transfer, denoted CT, as a reference. It is a complex parameter, and its relationship to ligand properties is not self-evident; we considered five possible expressions:
  - (i) the ionization potential of the ligand: the highest occupied molecular orbital energy  $E(\text{HOMO})$ , if Koopman's theorem is adopted
  - (ii) the inverse of the ionization potential of the ligand:  $1/E(\text{HOMO})$
  - (iii) the hardness of the ligand:  $\eta = \text{abs}(E(\text{HOMO}) - E(\text{LUMO}))/2$
  - (iv) the inverse of the hardness of the ligand:  $1/\eta$
  - (v) the ionization potential difference  $\Delta\text{IP} = E(\text{HOMO}_L) - E(\text{HOMO}_{\text{UO}_2^{2+}})$

The first problem was to choose the distance  $r$ . As we do not wish to take the optimized B3LYP distance, since this value becomes available only after the rather lengthy calculations that we wish to avoid, we decided to fix one distance for each coordination atom type based on van der Waals' radii for the neutral ligands. For the anionic ligands, we reduced the values by 0.2 Å because of the charge; this value was suggested by comparison with optimized distances involving neutral and anionic ligands (see Table 1). The values of the parameters  $r$  for each atom type are given in Table 3.

In Table 4, we present our results for 22 different fits of the coordination energy to different combinations of the parameters given above. The first case contains the three parameters  $\text{DM}/r^2$ ,  $q/r$ , and  $\text{POL}/r^4$ , which were found to be necessary to reproduce the largest part of the coordination energy. In cases 2 and 3, the PA and the REP parameters are added. From cases

**TABLE 4: Statistical Results for the Whole Ligand Set (Neutral and Anionic): Parameters Used, Correlation Coefficient, Coordination Energy Estimates for  $[\text{UO}_2(\text{acetone})_2]^{2+}$  and  $\text{UO}_2\text{Cl}_2$  Complexes (kJ/mol) with the Error in Comparison with the B3LYP Value, and  $t$ -Statistics Success**

case	parameters	corr coeff	rms	acetone	% err acetone	$\text{Cl}^-$	% err $\text{Cl}^-$	$t$ stat > 1
1	DM/ $r^2$ POL/ $r^4$ $q/r$	0.9480	222	967	22.1	1824	-12.7	+++
2	DM/ $r^2$ POL/ $r^4$ $q/r$ PA	0.9911	94	790	-0.3	1973	-5.6	++++
3	DM/ $r^2$ POL/ $r^4$ $q/r$ PA REP	0.9932	84	784	-1.0	2384	14.1	++++
4	DM/ $r^2$ POL/ $r^4$ $q/r$ PA CT	0.9936	82	793	0.1	1999	-4.3	++++
5	DM/ $r^2$ POL/ $r^4$ $q/r$ PA HOMO	0.9940	80	803	1.4	1982	-5.1	+ - +++
6	DM/ $r^2$ POL/ $r^4$ $q/r$ PA 1/HOMO	0.9915	94	795	0.4	1948	-6.7	++++
7	DM/ $r^2$ POL/ $r^4$ $q/r$ PA $\eta$	0.9940	79	805	1.6	1987	-4.9	+ - +++
8	DM/ $r^2$ POL/ $r^4$ $q/r$ PA 1/ $\eta$	0.9916	94	797	0.6	1956	-6.4	++++
9	DM/ $r^2$ POL/ $r^4$ $q/r$ PA $\Delta\text{IP}$	0.9932	85	817	3.2	1993	-4.6	++++
10	DM/ $r^2$ POL/ $r^4$ $q/r$ PA REP CT	0.9938	82	789	-0.4	2001	-4.2	++++
11	DM/ $r^2$ POL/ $r^4$ $q/r$ PA REP HOMO	0.9940	81	794	0.3	1985	-5.0	+ - +++
12	DM/ $r^2$ POL/ $r^4$ $q/r$ PA REP 1/HOMO	0.9939	81	791	-0.1	1957	-6.3	++++
13	DM/ $r^2$ POL/ $r^4$ $q/r$ PA REP $\eta$	0.9940	81	803	1.4	1988	-4.8	+ - +++
14	DM/ $r^2$ POL/ $r^4$ $q/r$ PA REP 1/ $\eta$	0.9941	80	793	0.1	1970	-5.7	++++
15	DM/ $r^2$ POL/ $r^4$ $q/r$ PA REP $\Delta\text{IP}$	0.9939	81	805	1.6	2000	-4.3	++++
16	DM/ $r^2$ POL/ $r^4$ $q/r$ REP	0.9652	186	893	12.8	1860	-11.0	+++
17	DM/ $r^2$ POL/ $r^4$ $q/r$ REP CT	0.9907	98	816	3.0	1996	-4.5	++++
18	DM/ $r^2$ POL/ $r^4$ $q/r$ REP HOMO	0.9665	186	866	9.3	1879	-10.1	+++ -
19	DM/ $r^2$ POL/ $r^4$ $q/r$ REP 1/HOMO	0.9655	189	907	14.5	1847	-11.6	+++ -
20	DM/ $r^2$ POL/ $r^4$ $q/r$ REP $\eta$	0.9666	186	863	9.0	1876	-10.2	+ + + -
21	DM/ $r^2$ POL/ $r^4$ $q/r$ REP 1/ $\eta$	0.9666	186	902	13.9	1835	-12.2	++++
22	DM/ $r^2$ POL/ $r^4$ $q/r$ REP $\Delta\text{IP}$	0.9901	102	864	9.1	1990	-4.7	++++
	B3LYP			792		2089		

4 to 9, the parameters are DM/ $r^2$ ,  $q/r$ , POL/ $r^4$ , PA, and various charge-transfer expressions. From cases 10 to 15, the repulsion term is added, and from cases 16 to 22, the PA parameter is removed while the repulsion term is kept. The table also gives the correlation coefficient, the root-mean-square (rms) error, and the  $t$ -statistics of the regression.

It is not necessary to analyze exhaustively each row of Table 4. We observe that the correlation coefficient is always greater than 0.9 and frequently greater than 0.99. In a statistical sense, the correlation is, therefore, always good and frequently very good. To test the different sets of parameters, the coordination energies of two complexes not in the database ( $[\text{UO}_2(\text{acetone})_2]^{2+}$  and  $\text{UO}_2\text{Cl}_2$ ) have been estimated. The estimates are given in Table 4, together with their errors (i.e., the differences between the statistical estimates and the B3LYP values). With a judicious choice of parameters, the estimates are remarkably accurate for  $[\text{UO}_2(\text{acetone})_2]^{2+}$  (errors frequently less than 1%) while the error for  $\text{UO}_2\text{Cl}_2$ , though larger at about 5% in favorable cases, is still acceptable. The whole study shows that three of the parameters,  $q/r$ , DM/ $r^2$ , and POL/ $r^4$ , are essential to obtain a good estimate. The results concerning the proton affinity, repulsion, and charge-transfer parameters are not very easy to understand. We note that the fits are better when the proton affinity parameter is added in the statistical study: compare, for example, cases 1 and 2.

To evaluate the statistical significance of a particular parameter, we looked at the  $t$  value. In a statistical study, if  $t$  is smaller than 1 for a parameter, we can say that the parameter is nonsignificant. In these cases the sign - appears in the last column in Table 4. In Figure 2, the  $t$ -statistics are plotted for cases 10–15. It can be seen that the charge parameter gives the most significant contribution to the coordination energy ( $t$ -statistics always greater than 10). This observation is not unexpected; it merely reflects the large electrostatic component of the bonding between an anion and the uranyl dication.

Cases 10–15 enable us to evaluate the five different charge-transfer expressions. To reproduce the DFT data, the best graph is the one which is most similar to that with the CT parameter. The best of the five parameters is seen to be  $\Delta\text{IP}$ , which is the difference between the ionization potentials of the

ligand and of  $\text{UO}_2^{2+}$ . It has a simple physical meaning because it represents the transfer of charge from the ligand to the uranyl ion: the HOMO energy of the ligand represents the ionization potential of the ligand (the capacity to lose an electron), and the HOMO energy of  $\text{UO}_2^{2+}$  represents the electronic affinity of  $\text{UO}_2^{2+}$  (the capacity to gain an electron). We have not been able to find a parameter linked only to the ligand that is able to represent the charge transfer correctly.

The  $t$ -statistic for the PA parameter is highly variable (see Figure 2), and its contribution to the coordination energy ranges from large to rather small. These graphs raise an important question: can we attach a physical meaning to the proton affinity in our study? We consider this point in detail below.

To eliminate any statistical “noise” caused by the numerically large binding energies of anionic ligands, we decided to undertake some statistical tests of a reduced ligand set containing only neutral molecules. It seems clear that any treatment cycle proposed for nuclear waste would be based on neutral ligands. Results of these tests are reported in Table 5. Various combinations of parameters were tested to evaluate the coordination energy of  $[\text{UO}_2(\text{acetone})_2]^{2+}$ . The results do not differ significantly from those obtained in the study with the complete ligand set. The parameter  $\Delta\text{IP}$  is always the best representation of the charge transfer, the PA seems to be necessary to obtain good estimates, and the most accurate estimate is given by case 8, which corresponds to case 15 in Table 4.

We now consider the physical meaning of each component of the binding energy. We analyze the value of the different contributions for  $[\text{UO}_2(\text{H}_2\text{O})_2]^{2+}$  and  $\text{UO}_2\text{F}_2$  (Table 6) in each statistical case, for the whole set, with the CEP values as a reference. These two examples are considered as typical cases of neutral and anionic ligands, respectively. We would be satisfied if the results of the CEP analysis are reproduced semiquantitatively by a statistical fit. We do not expect to be able to obtain exact agreement, since the CEP data are obtained from SCF calculations whereas the statistical results are fitted to B3LYP energies. However, the SCF and B3LYP ligand binding energies are rather similar; the SCF values are smaller but only by 3% for  $\text{UO}_2\text{F}_2$  or 8% for  $[\text{UO}_2(\text{H}_2\text{O})_2]^{2+}$ . In some cases, an apparently successful statistical fit is obtained even

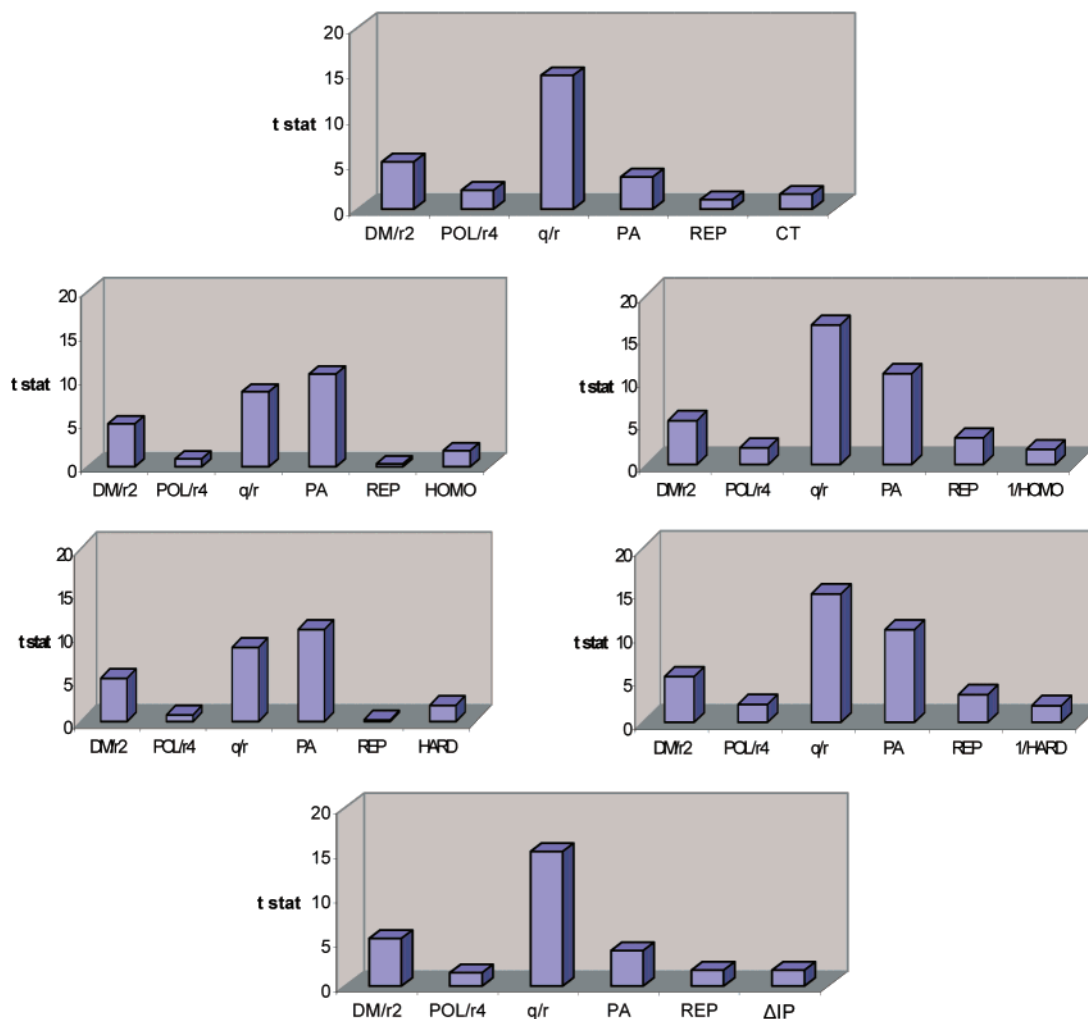


Figure 2.  $t$ -statistics for cases 10–15 in the statistical study.

TABLE 5: Statistical Results for the Neutral Ligand Set: Parameters Used, Correlation Coefficient, Coordination Energy Estimates for  $[\text{UO}_2(\text{acetone})_2]^{2+}$  Complex (kJ/mol) with the Error in Comparison with the B3LYP Value,  $t$ -Statistics Success

case	parameters	corr coeff	rms	acetone	% err acetone	$t$ stat > 1
1	DM/ $r^2$ POL/ $r^4$	0.5039	188	1003	26.6	++
2	DM/ $r^2$ POL/ $r^4$ PA	0.9685	55	835	5.4	+++
3	DM/ $r^2$ POL/ $r^4$ REP	0.7402	150	932	17.7	+++
4	DM/ $r^2$ POL/ $r^4$ REP CT	0.9349	81	851	7.4	++++
5	DM/ $r^2$ POL/ $r^4$ REP $\Delta$ IP	0.9413	77	897	13.3	++++
6	DM/ $r^2$ POL/ $r^4$ PA REP	0.9830	42	827	4.4	++++
7	DM/ $r^2$ POL/ $r^4$ PA REP CT	0.9832	43	827	4.4	++++-
8	DM/ $r^2$ POL/ $r^4$ PA REP $\Delta$ IP	0.9858	39	837	5.7	+++++
	B3LYP			792		

though individual components are completely nonphysical. For example, in cases 6, 12, and 19, a strongly *repulsive* contribution to the binding is predicted for the charge-transfer component for  $\text{UO}_2\text{F}_2$  and an essentially *zero contribution* for  $[\text{UO}_2(\text{H}_2\text{O})_2]^{2+}$ . In several cases (17–22), the repulsion energy is apparently *attractive*. Quantitatively, the contribution for the polarization term is too small in every single statistical fit for both  $\text{UO}_2\text{F}_2$  and  $[\text{UO}_2(\text{H}_2\text{O})_2]^{2+}$ , and often by large amounts. Similarly, the electrostatic component ( $q/r$  for  $\text{UO}_2\text{F}_2$  and DM/ $r^2$  for  $[\text{UO}_2(\text{H}_2\text{O})_2]^{2+}$ ) is always too small, again often to a large extent. We are forced to a rather disappointing conclusion: no set of our parameters yields a physically sensible energy decomposition. This conclusion is also valid for the reduced ligand set containing neutral molecules.

To determine which of our parameters are statistically independent, we have carried out a principal component analysis

(PCA). Table 7 gives the resulting correlation matrices for cases 1, 2, 10, and 22. As the proton affinity and charge parameters are highly correlated, it is clear that their contributions to the binding energy are not statistically independent. In other words, these parameters do not satisfy the requirements we set. The same remark is possible for the NBO charge transfer or the  $\Delta$ IP parameter with or without the presence of the proton affinity.

To conclude this statistical study, we have shown that a simple linear regression is an effective way to estimate the coordination energy of a new complex with two ligands. We do not claim that our binding-energy estimates will necessarily be appropriate for complexes containing a different number of ligands. Unfortunately, this statistical method does not allow us to obtain “the right answer for the right reason”, because the decomposition of the individual terms is clearly unsound. Where are the inadequacies in our statistical treatment? We suspect that the

**TABLE 6: Statistical and Coordination Energy Partitioning Values of the Coordination Energy Components for  $[\text{UO}_2(\text{H}_2\text{O})_2]^{2+}$  (First Row) and  $\text{UO}_2\text{F}_2$  (Second Row) (Energies in kJ/mol), and the Electrostatic Term (Third Column) Represented as  $\text{DM}/r^2$  for  $[\text{UO}_2(\text{H}_2\text{O})_2]^{2+}$  and  $q/r$  for  $\text{UO}_2\text{F}_2$** 

case	residual	ELEC	POL/ $r^4$	PA	charge transfer							
					CT	HOMO	1/HOMO	$\eta$	1/ $\eta$	$\Delta\text{IP}$	REP	
CEP		404	96		138							-148
		2542	252		268							-853
1	175	298	77									
	215	2077	125									
2	-19	130	71	427								
	86	1370	115	939								
3	13	146	13	539								-159
	123	1282	21	1185								-194
4	24	150	17	288	71							
	136	1437	28	634	182							
5	-11	139	7	573		-157						
	76	1069	11	1261		-1						
6	-17	132	15	422			-0.5					
	1	1355	24	929			-109					
7	-12	142	6	576				-161				
	71	1073	9	1268				-5				
8	-16	132	15	414					5			
	-10	1326	25	912					164			
9	-12	153	11	260							139	
	100	1243	18	573							483	
10	-27	152	16	383	50							-77
	139	1375	26	843	128							-94
11	-6	141	7	576		-136						-31
	85	1091	12	1267		-1						-37
12	19	150	15	545			-0.8					-178
	-1	1249	24	1199			-163					-217
13	-9	143	6	578				-148				-19
	76	1086	10	1271				-4				-23
14	21	151	16	535					7			-177
	-8	1210	25	1176					230			-217
15	8	157	12	389							96	-111
	121	1221	19	857							335	-135
16	24	189	47									-292
	85	1899	77									-356
17	55	170	27		146							152
	163	1650	43		374							186
18	44	191	51			158						107
	133	2072	83			1						130
19	27	192	49					-0.4				284
	14	1884	79					-94				347
20	47	188	52						170			93
	142	2072	85						5			114
21	34	194	50							8		265
	-75	1804	81							284		323
22	1	186	15								280	69
	111	1224	24								974	84

weakest link concerns the treatment of charge transfer, which has been shown to depend on overlap factors unique to each ligand.<sup>18</sup> It may also be that a representation of Pauli repulsion by a simple exponential formula is inadequate. Further work is planned in this area.

**(3) Contributions to the Interaction Energy.** (a)  $[\text{UO}_2\text{H}_2\text{O}]^{2+}$  and  $[\text{UO}_2\text{H}_2\text{S}]^{2+}$ . For all the complexes studied, the CEP gives us the various contributions that need to be modeled in order to be introduced in a force field. We have already shown that if the uranyl ion is replaced by a point charge +2 in  $[\text{UO}_2(\text{H}_2\text{O})]^{2+}$  and  $[\text{UO}_2(\text{H}_2\text{S})]^{2+}$  complexes, quantitatively correct results for the coordination energy are obtained with this remarkably simple model.<sup>2c</sup> We decided to extend this study by undertaking CEP calculations at varying U–O and U–S distances.

(i) *H<sub>2</sub>O Ligand.* To model the electrostatic contribution, we used a multipole development. Because of the interaction along the dipole moment direction of the water molecule, the first term of the development  $q^*\mu/r^2$  will be the largest and all the

other terms will be negligible, since the components of the quadrupole moment are small in the water molecule. In Figure 3, we plot the electrostatic term derived from the CEP calculations and from two numerical models intended to reproduce this term that are described below.

The expression  $q^*\mu/r^2$  overestimates the magnitude of the electrostatic term at short distance, because of the non-negligible charge transfer from the ligand to  $\text{UO}_2^{2+}$ . In fact, the uranyl ion is not really a +2 charge if the charge transfer does not equal zero. A better approach is to decrease the charge by the quantity “%CT”:

$$\%CT = \frac{\text{CT}}{\text{ELEC} + \text{POL} + \text{CT}} \times 100$$

where  $\text{ELEC} + \text{POL} + \text{CT}$  is the sum of the attractive contributions.

Thus, the uranyl charge, as a function of the distance  $r$ , becomes  $q_{\text{CT}}(r) = 2 - \%CT(r)/100$ . As can be seen in Figure



**TABLE 7: Correlation Matrices in Principal Component Analysis**

parameter	$E_c$	$\text{DM}/r^2$	$\text{POL}/r^4$	$q/r$
$E_c$	1			
$\text{DM}/r^2$	-0.095	1		
$\text{POL}/r^4$	0.100	0.341	1	
$q/r$	-0.955	0.282	0.073	1

parameter	$E_c$	$\text{DM}/r^2$	$\text{POL}/r^4$	$q/r$	PA
$E_c$	1				
$\text{DM}/r^2$	-0.095	1			
$\text{POL}/r^4$	0.100	0.341	1		
$q/r$	-0.955	0.282	0.073	1	
PA	0.965	-0.110	0.180	-0.893	1

parameter	$E_c$	$\text{DM}/r^2$	$\text{POL}/r^4$	$q/r$	PA	REP	CT (NBO)
$E_c$	1						
$\text{DM}/r^2$	-0.095	1					
$\text{POL}/r^4$	0.100	0.341	1				
$q/r$	-0.955	0.282	0.073	1			
PA	0.965	-0.110	0.180	-0.893	1		
REP	0.218	0.177	0.158	-0.252	0.144	1	
CT (NBO)	0.644	-0.181	0.055	-0.541	0.693	-0.471	1

parameter	$E_c$	$\text{DM}/r^2$	$\text{POL}/r^4$	$q/r$	REP	$\Delta\text{IP}$
$E_c$	1					
$\text{DM}/r^2$	-0.095	1				
$\text{POL}/r^4$	0.100	0.341	1			
$q/r$	-0.955	0.282	0.073	1		
REP	0.218	0.177	0.158	-0.252	1	
$\Delta\text{IP}$	-0.934	0.222	-0.117	0.882	-0.056	1

3, this expression  $q_{\text{CT}}\mu/r^2$  gives a very satisfactory representation of the electrostatic contribution even for U–O distances as short as 2 Å, which is less than the equilibrium distance.

To model the polarization term, we have used the formulation with the electrical field (second-order perturbation theory)  $q^2\alpha/(2r^4)$ , where  $\alpha$  is the dipole polarizability of  $\text{H}_2\text{O}$ . Our results are presented in Figure 4. As Gresh et al.<sup>26</sup> have already shown, a cation cannot be successfully modeled by a +2 point charge at short distances. It is rather unusual to attempt to model the charge-transfer contribution, and this term is not often present in force fields. It is known that the charge transfer behaves as an exponential function of the distance.<sup>27</sup> We have also fitted the CEP charge transfer by the expression  $a \exp(-br)$ , and it seems to be a good model (see Figure 5). Our next task is to analyze the  $\sigma$  and  $\pi$  charge transfers and to evaluate their variations with the angle of approach of the water molecule. CEP calculations allow that partitioning, and the results will be presented elsewhere.

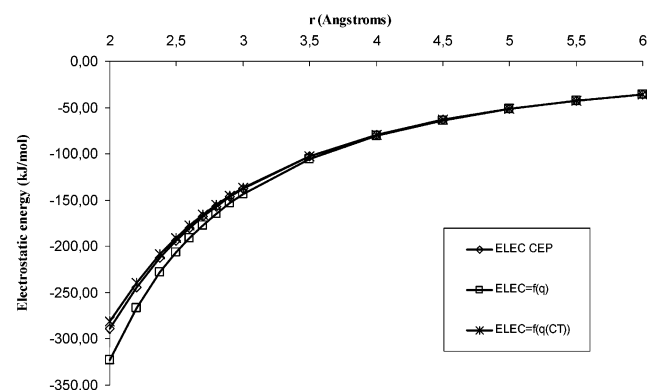


**Figure 3.** Variation of the electrostatic component with the uranyl–water distance. CEP calculations and the two models (with a +2 charge and the charge as a function of the charge transfer) are plotted.

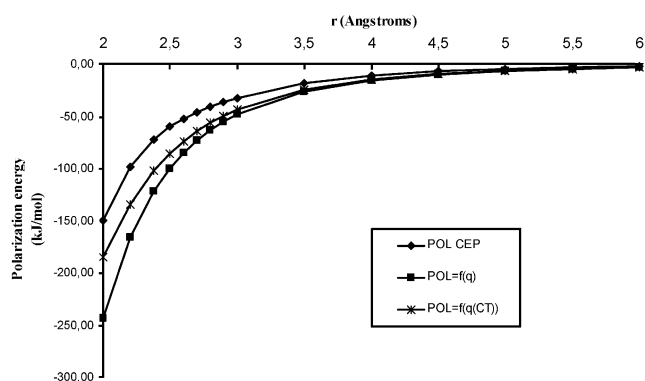


**Figure 4.** Variation of the polarization component with the uranyl–water distance. CEP calculations and the two models (with a +2 charge and the charge as a function of the charge transfer) are plotted.

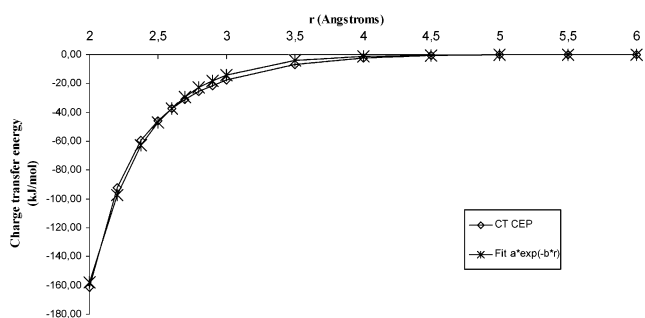


**Figure 5.** Variation of the charge-transfer component with the uranyl–water distance. CEP calculations and the exponential fit are plotted.

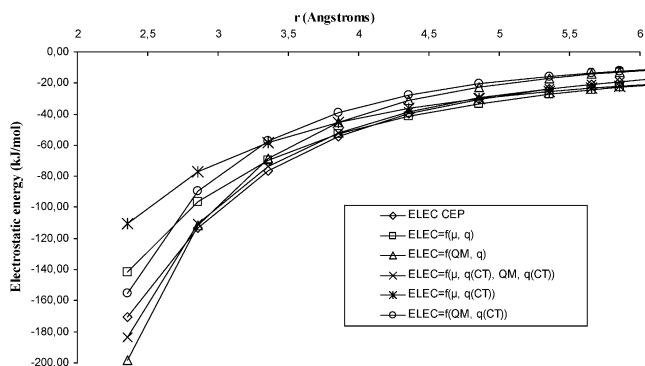


**Figure 6.** Variation of the electrostatic component with the uranyl– $\text{H}_2\text{S}$  distance. CEP calculations and the five models are plotted.

(ii)  $\text{H}_2\text{S}$  Ligand. The same models have been applied to the  $[\text{UO}_2(\text{H}_2\text{S})]^{2+}$  complex to reproduce the CEP contributions: electrostatic, polarization, and charge transfer.

For the electrostatic contribution, Figure 6 gives the variation of the CEP data and five different models. The  $[\text{UO}_2\text{H}_2\text{S}]^{2+}$  geometry is different from the structure of the water complex.  $\text{H}_2\text{O}$  has a large dipole moment which favors a  $C_{2v}$  structure, but  $\text{H}_2\text{S}$  has a small dipole moment and a strong quadrupole moment component, perpendicular to the dipole moment; this quadrupole contribution to the electrostatic component is therefore largest if the  $\text{H}_2\text{S}$  plane is perpendicular to the uranyl axis, which leads to a  $C_s$  structure. In fact, the structure is a compromise where the angle between the  $\text{O}_2\text{US}$  and  $\text{SH}_2$  planes is  $70^\circ$ . Thus, the expression  $q^*\mu/r^2$  underestimates the ab initio results for distances less than 4 Å, and even the expression  $q_{\text{CT}}\mu/r^2$  is not an improvement in this case. To test whether the dipole moment contribution is negligible, two expressions describing the interaction with the quadrupole moment ( $Q$ ) have been tested:  $qQ/(3r^3)$  and  $q_{\text{CT}}Q/(3r^3)$ . However, these relationships

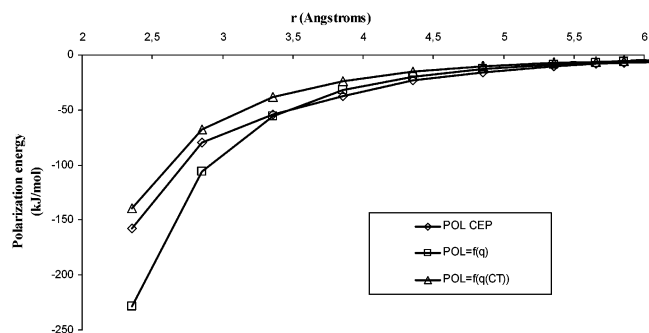


**Figure 7.** Variation of the polarization component with the uranyl–H<sub>2</sub>S distance. CEP calculations and the two models (with a +2 charge and the charge as a function of the charge transfer) are plotted.

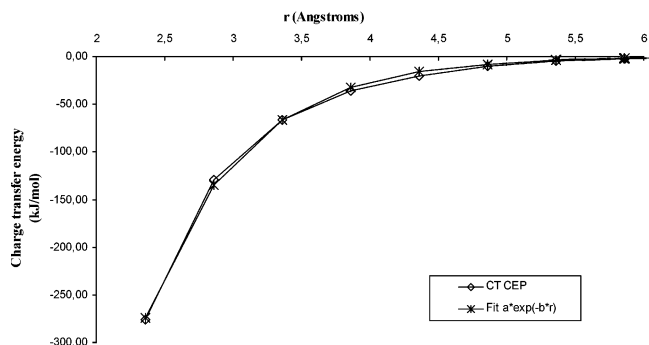


**Figure 8.** Variation of the charge-transfer component with the uranyl–H<sub>2</sub>S distance. CEP calculations and the exponential fit are plotted.

overestimate the electrostatic term at short distances. The last model takes into account both the dipole-moment and quadrupole-moment components (with the charge expressed as a function of the charge transfer):

$$\text{ELEC} = \frac{q_{\text{CT}}^2}{r^2} \cos(70^\circ) + \frac{q_{\text{CT}}Q}{3r^2} \sin(70^\circ)$$

As can be seen in Figure 6, this model gives a successful representation of the electrostatic contribution, with the added advantage that it is physically meaningful. To model the polarization term, we have used the same models tested for H<sub>2</sub>O (Figure 7). The results obtained using the  $q_{\text{CT}}$  function are not quite as accurate as those in the case of water. We suspect an effect of a higher-order term of the polarizability.

In Figure 8, we have fitted the ab initio charge transfer by an exponential expression, and as for the H<sub>2</sub>O complex, this expression is successful. Quantitatively, the charge transfer is more important for [UO<sub>2</sub>(H<sub>2</sub>S)]<sup>2+</sup> than for [UO<sub>2</sub>(H<sub>2</sub>O)]<sup>2+</sup> (130 and 60 kJ/mol at the equilibrium distance, respectively). A simple explanation is given by the ionization potentials of the two ligands, if Koopman's theorem is accepted. The H<sub>2</sub>S HOMO energy is less negative (−7.23 eV) than that for H<sub>2</sub>O (−8.69 eV), favoring the electron transfer from the ligand to the uranyl ion (see Table 2).

(b) UO<sub>2</sub>L<sub>2</sub><sup>n+</sup> (*n* = 0, 2). CEP calculations have been performed for several UO<sub>2</sub>L<sub>2</sub><sup>n+</sup> complexes where L are simple model ligands to understand the interaction with several types of binding sites: H<sub>2</sub>O, H<sub>2</sub>S, F<sup>−</sup>, H<sub>2</sub>, and NH<sub>3</sub>.

Table 8 gives the various contributions. First, we note that inverse charge transfer (from uranyl to ligand) is negligible in all these complexes. We have already drawn attention to the very high electron affinity of the uranyl ion. Conversely, the polarization of UO<sub>2</sub><sup>2+</sup> is not negligible because of its substantial polarizability (40 au<sup>3</sup>). For the other contributions, it is necessary

**TABLE 8: Coordination Energy Partitioning for Several UO<sub>2</sub>L<sub>2</sub><sup>n+</sup> Complexes (L = H<sub>2</sub>O, H<sub>2</sub>S, HCl, F<sup>−</sup>, NH<sub>3</sub>): Electrostatic, Polarization of the Ligand, Charge Transfer from the Ligand to the Uranyl Ion, Polarization of the Uranyl Ion, and Inverse Charge Transfer Contributions**

L	ELEC	REP	POL(L)	CT(L)	POL(U)	CT(U)	total
H <sub>2</sub> O	404	−148	48	69	16	0	389
H <sub>2</sub> S	206	−166	90	86	3	4	223
HCl	136	−193	76	83	5	0	107
H <sub>2</sub>	20	−48	26	35	3	0	36
F <sup>−</sup>	2542	−853	126	134	138	1	2088
NH <sub>3</sub>	482	−189	63	69	16	2	443

to separate neutral from charged ligands. For F<sup>−</sup>, the electrostatic term is the largest because of the charge–charge interaction, and all the other attractive contributions can be neglected. This observation justifies the success of a simple point-charge model already noted by Ismail et al.<sup>2b</sup> For neutral ligands, we note that the electrostatic contribution is significant but it does not dominate the other attractive terms. The sum of ligand polarization and ligand-to-uranyl charge transfer is at least 20% of the sum of the attractive terms, and it amounts to as much as 53% for HCl, for example. We conclude that these polarization and charge-transfer terms need to be taken into account in model potentials to reproduce structures and chemical bonding properties accurately, despite the implementation difficulties.

If we compare H<sub>2</sub>O and H<sub>2</sub>S complexes, the U–S distance is of course longer than the U–O(water) distance, and we have already compared the dipole moments. In [UO<sub>2</sub>(H<sub>2</sub>S)<sub>2</sub>]<sup>2+</sup>, the hydrogen atoms' orientation is the same as that in the single ligand complex, due to the quadrupole moment contribution. The U–S distance and the H<sub>2</sub>S orientation explain why the electrostatic contribution is smaller for [UO<sub>2</sub>(H<sub>2</sub>S)<sub>2</sub>]<sup>2+</sup> than for the analogous water complex. The high polarizability of H<sub>2</sub>S accounts for the large polarization energy (see Table 2). The lower ionization potential of H<sub>2</sub>S leads to enhanced charge transfer, despite the longer distance, and this phenomenon is confirmed by the NBO values: 0.53 electron transferred for H<sub>2</sub>S but only 0.25 for H<sub>2</sub>O.

The comparison of the electrostatic term between H<sub>2</sub>S and HCl complexes is rather subtle; HCl has a larger dipole moment but a smaller electrostatic energy, although the distances are very similar. Once again, the quadrupole moments provide the explanation. Indeed, we notice the same kind of geometry orientation in the two complexes; as the dipole moments of these two complexes are almost perpendicular to the uranyl–ligand direction (70° for both H<sub>2</sub>S and HCl), the electrostatic energy due to the dipole moment is rather small for both H<sub>2</sub>S and HCl. The quadrupole moment perpendicular to the dipole moment is larger than that parallel, which favors the approximately perpendicular orientation of the ligand. Since the perpendicular quadrupole moment is larger in H<sub>2</sub>S than that for HCl, the electrostatic binding energy is more important in the H<sub>2</sub>S complex. The comparison of the polarization and charge-transfer contributions is straightforward and consistent with the polarizabilities, ionization potentials, and NBO values. We have already drawn attention to the different geometries of the [UO<sub>2</sub>(HCl)<sub>2</sub>] and [UO<sub>2</sub>(HF)<sub>2</sub>] complexes (section III.1). The U–F–H angle is almost linear, since in this case its quadrupole moment is much smaller than that for HCl whereas the dipole moment is larger.

The [UO<sub>2</sub>(H<sub>2</sub>)<sub>2</sub>]<sup>2+</sup> complex is very different; since H<sub>2</sub> does not have a dipole moment and the quadrupole moment components are small, the electrostatic contribution is not dominant and the sum POL(L) + CT(L) represents 73% of the attractive terms. This system reinforces the point already made

above on the importance of treating polarization and charge transfer, and it emphasizes the necessity to use a multipole electrostatic description to model symmetric and neutral molecules.

The comparison between  $\text{NH}_3$  and  $\text{H}_2\text{O}$  complexes shows, once again, the need to consider the quadrupole moment in order to understand the electrostatic terms. In fact, the dipole moment is smaller for  $\text{NH}_3$  than for  $\text{H}_2\text{O}$ , but the quadrupole moment component in the dipole moment direction is larger, and the addition of these two effects leads to the larger electrostatic contribution for the  $\text{NH}_3$  complex.  $\text{NH}_3$  is more polarizable than  $\text{H}_2\text{O}$  (Table 2), and therefore, the polarization energy is larger. The charge-transfer contributions are the same for the two complexes; the influence of a higher ionization potential for the water molecule is canceled by a shorter bond distance in the water complex.

To conclude, we emphasize that the binding energies and geometries of uranyl complexes can be successfully reproduced only if we model the electrostatic contribution accurately by a multipole development and if the ligand polarization and the ligand-to-uranyl charge transfer contributions are properly represented. We can summarize our analysis of the uranyl–ligand interactions as follows. While the electrostatic term is the largest component of the binding energy, the contributions from ligand polarization and ligand-to-uranyl charge transfer are both significant; consideration of the properties of individual ligands enables us to understand the variation in binding energies in terms of physically meaningful quantities. Analytical expressions that describe the components of the binding energy have been developed and successfully tested.

#### (IV) Conclusions

We have undertaken an extensive theoretical survey of uranyl complexes containing both neutral and anionic ligands. No experimental coordination energies for these complexes are currently available. We have shown that a statistical study of the QSAR type is able to estimate the coordination energy of a new complex with an error of the order of 5%; it is unlikely that the error in DFT calculations is smaller than this. The statistical method gives the energetic contributions of each parameter to the coordination energy, but no set of parameters could be found which is physically meaningful. The CEP method, based on an RVS decomposition, is able to yield a quantitative analysis of the chemical interaction between the uranyl ion and several different ligands. The bonding properties of different ligands can, therefore, be compared in detail. This method gives precise and physically meaningful contributions to the binding energy; various model expressions have been tested to represent these contributions as a function of the ligand–uranium distance. If the charge of the uranyl ion is reduced to allow for charge transfer, the polarization and the electrostatic terms can be reproduced accurately. Both the dipole moment and quadrupole moment contributions must be considered to reproduce the electrostatic contribution. The charge transfer has been successfully fitted by an exponential function of the uranyl–ligand distance. In current work, a classical model potential built from these expressions is being used to study not only water complexes of the uranyl ion with explicit consideration of the first, second, and third coordination spheres but also these complexes in aqueous solution.

**Acknowledgment.** We would like to thank Philippe Millié for fruitful discussions about the statistical study and Yannick

Carissan for helpful technical assistance concerning the implementation of the CEP procedure in Molcas. We thank the CINES for a generous allocation of computing resources (project pqt1073), and the GdR PRACTIS for financial support.

#### References and Notes

- (1) (a) Bardin, N.; Rubini, P.; Madic, C. *Radiochim. Acta* **1998**, *83*, 189. (b) Quilès, F.; Burneau, A. *Vib. Spectrosc.* **1998**, *18*, 61. (c) Aberg, M.; Ferri, D.; Glaser, J.; Grenthe, I. *Inorg. Chem.* **1983**, *22*, 3986. (d) Wahlgren, U.; Moll, H.; Schimmelpfennig, B.; Maron, L.; Vallet, V.; Groppen, O. *J. Phys. Chem. A* **1999**, *103*, 8257. (e) Allen, P. G.; Bucher, J. J.; Shuh, D. K.; Edelstein, N. M.; Reich, T. *Inorg. Chem.* **1997**, *36*, 4676.
- (2) (a) Straka, M.; Dyllal, K. G.; Pyykkö, P. *Theor. Chem. Acc.* **2001**, *106*, 393. (b) Ismail, N.; Marsden, C.; Baerends, E. J. Manuscript in preparation. (c) Ismail, N.; Marsden, C. Manuscript in preparation. (d) Schreckenbach, G.; Hay, P. J.; Martin, R. L. *J. Comput. Chem.* **1999**, *20*, 70. (e) Hay, P. J.; Martin, R. L.; Schreckenbach, G. *J. Phys. Chem. A* **2000**, *104*, 6259.
- (3) Hemmingsen, L.; Amara, P.; Ansoborlo, E.; Field, M. J. *J. Phys. Chem. A* **2000**, *104*, 4095.
- (4) (a) Guilbaud, P.; Wipff, G. *J. Phys. Chem.* **1993**, *97*, 5685. (b) Guilbaud, P.; Wipff, G. *J. Mol. Struct.* **1996**, *366*, 55.
- (5) Pearlman, D. A.; Case, D. A.; Cadwell, J. C.; Seibel, G. L.; Singh, U. C.; Weiner, P.; Kollman, P. A. *AMBER 4*; University of California, San Francisco, CA, 1991.
- (6) Reed, A. E.; Curtiss, L. A.; Weinhold, F. *Chem. Rev.* **1988**, *88*, 899.
- (7) Becke, A. D. *J. Chem. Phys.* **1993**, *98*, 5648.
- (8) Boys, S. F.; Bernardi, F. *Mol. Phys.* **1970**, *19*, 553.
- (9) Frisch, M. J.; Trucks, G. W.; Schlegel, H. B.; Scuseria, G. E.; Robb, M. A.; Cheeseman, J. R.; Zakrzewski, V. G.; Montgomery, J. A., Jr.; Stratmann, R. E.; Burant, J. C.; Dapprich, S.; Millam, J. M.; Daniels, A. D.; Kudin, K. N.; Strain, M. C.; Farkas, O.; Tomasi, J.; Barone, V.; Cossi, M.; Cammi, R.; Mennucci, B.; Pomelli, C.; Adamo, C.; Clifford, S.; Ochterski, J.; Petersson, G. A.; Ayala, P. Y.; Cui, Q.; Morokuma, K.; Malick, D. K.; Rabuck, A. D.; Raghavachari, K.; Foresman, J. B.; Cioslowski, J.; Ortiz, J. V.; Baboul, A. G.; Stefanov, B. B.; Liu, G.; Liashenko, A.; Piskorz, P.; Komaromi, I.; Gomperts, R.; Martin, R. L.; Fox, D. J.; Keith, T.; Al-Laham, M. A.; Peng, C. Y.; Nanayakkara, A.; Gonzalez, C.; Challacombe, M.; Gill, P. M. W.; Johnson, B. G.; Chen, W.; Wong, M. W.; Andres, J. L.; Head-Gordon, M.; Replogle, E. S.; Pople, J. A. *Gaussian 98*, Revision A.9; Gaussian, Inc.: Pittsburgh, PA, 1998.
- (10) A.; Carissan, Y.; Cooper, D. L.; Fleig, T.; Fülcher, M. P.; Gagliardi, L.; de Graaf, C.; Hess, B. A.; Karlström, G.; Lindh, R.; Malmqvist, P.-Å.; Neogrády, P.; Olsen, J.; Roos, B. O.; Schimmelpfennig, B.; Schütz, M.; Seijo, L.; Serrano-Andrés, L.; Siegbahn, P. E. M.; Ståhlberg, P. E. M.; Thorsteinsson, T.; Velyazov, V.; Wierzbowska, M.; Widmark, P.-O. *MOLCAS*, Version 3; University of Lund: Sweden, 2001.
- (11) Ismail, N.; Heully, J.-L.; Saue, T.; Daudey, J.-P.; Marsden, C. J. *Chem. Phys. Lett.* **1999**, *300*, 296.
- (12) Kühle, W.; Dolg, M.; Stoll, H.; Preuss, H. *J. Chem. Phys.* **1994**, *100*, 7535.
- (13) (a) De Jong, W. A.; Visscher, L.; Nieuwport, W. C. *J. Mol. Struct. (THEOCHEM)* **1998**, *458*, 41. (b) De Jong, W. A.; Visscher, L.; Nieuwport, W. C. *J. Mol. Struct. (THEOCHEM)* **2002**, *581*, 259 (corrigendum).
- (14) Bouteiller, Y.; Mijoule, C.; Nizam, M.; Barthelat, J.-C.; Daudey, J.-P.; Pelissier, M.; Silvi, B. *Mol. Phys.* **1988**, *65*, 295.
- (15) Begner, A.; Dolg, M.; Kühle, W.; Stoll, H.; Preuss, H. *Mol. Phys.* **1993**, *80*, 1431.
- (16) (a) Fink, W. H. *J. Chem. Phys.* **1972**, *57*, 1822. (b) Stevens, W.; Fink, W. H. *Chem. Phys. Lett.* **1987**, *139*, 15.
- (17) Morokuma, K. *J. Chem. Phys.* **1971**, *55*, 1236.
- (18) Hoyau, S.; Brenner, V.; Granucci, G.; Millié, P.; Dognon, J. P. Manuscript in preparation.
- (19) Kaupp, M.; Schleyer, P. v. R. *J. Phys. Chem.* **1992**, *96*, 7316.
- (20) Derepas, A.-L.; Soudan, J. M.; Brenner, V.; Dognon, J.-P.; Millé, P. *J. Comput. Chem.* **2002**, *23*, 1013.
- (21) Pearson, R. G. *Coord. Chem. Rev.* **1990**, *100*, 403.
- (22) McKibben, J. M. *Radiochim. Acta* **1984**, *36*, 3.
- (23) Cornehl, H. H.; Heinemann, C.; Marçalo, J.; Pries de Matos, A.; Schwarz, H. *Angew. Chem.* **1996**, *108*, 950; *Angew. Chem., Int. Ed. Engl.* **1996**, *35*, 891.
- (24) Mulliken, R. S. *J. Chem. Phys.* **1955**, *23*, 1833.
- (25) Rabbe, C. Ph.D. Thesis, CEA, 1996.
- (26) (a) Garmer, D. R.; Gresh, N. *J. Am. Chem. Soc.* **1994**, *116*, 3556. (b) Gresh, N.; Stevens, W. J.; Krauss, M. *J. Comput. Chem.* **1995**, *16*, 843. (c) Gresh, N. *J. Comput. Chem.* **1995**, *16*, 856.
- (27) Stone, A. J. *Chem. Phys. Lett.* **1993**, *211*, 101.